Benzothiadiazole을 기본골격으로 한 공액형 올리고머 합성 및 유기태양전지 응용

신 웅 · 김윤환 · Nadhila Sylvianti · Mutia Anissa Marsya · Devi Saskia Putri · 문두경* · 김주현†

부경대학교 고분자공학과, *건국대학교 신소재공학과

(2016년 6월 19일 접수, 2016년 7월 12일 수정, 2016년 7월 16일 채택)

Synthesis of Conjugated Oligomer Based on Benzothiadiazole and Its Application of Organic Solar Cells

Woon Shin, Youn Hwan Kim, Nadhila Sylvianti, Mutia Anissa Marsya, Devi Saskia Putri,
Doo Kyung Moon*, and Joo Hyun Kim†

Department of Polymer Engineering, Pukyong National University, Busan 48547, Korea
Department of Materials Chemistry and Engineering, Konkuk Univerisity, Seoul 05029, Korea
(Received June 19, 2016; Revised July 12, 2016; Accepted July 16, 2016)

초록: 2,1,3-benzothiadiazole(BT)과 silofluorene(SiF)을 기본골격으로 하는 acceptor(A) - donor(D) - acceptor(A) 형태의 공액형(conjugated) 분자(SiF-BT)를 합성하였다. 공액결합의 길이를 늘여 주기 위하여 두 개의 thiophene을 SiF와 BT 사이에 도입하였으나 밴드갭은 꽤 큰 2.26 eV에 불과하였다. 이는 SiF와 BT 사이의 intramolecular charge transfer의 정도가 작기 때문이라 판단된다. 순환전압전류법 및 흡수분광법을 이용하여 측정한 SiF-BT의 HOMO 및 LUMO 에너지 준위는 각각 -5.43 and -3.17 eV이며, 최적화된 유기태양전지의 효율은 0.53%(단락전류=-2.06 mA/cm^2, 충진인자=29.8%, 개방전압=0.90 V)임을 확인하였다.

Abstract: Acceptor (A) - donor (D) - acceptor (A) type conjugated small molecule based on 2,1,3-benzothiadiazole and silofluorene (2,7-bis[5-(7-methyl-benzo[1,2,5]thiadiazol-4-yl)-thiophen-2-yl]-9-(9,9-dioctyl)-9H-silofluorene, SiF-BT) is synthesized for application in organic solar cells (OSCs). Even though two thiophene rings are introduced as the π-extender, SiF-BT exhibits a wide band gap of 2.26 eV due to weak intramolecular charge transfer between SiF and BT. The HOMO and LUMO energy levels of SiF-BT figured out from the cyclic voltammogram and UV-Visible spectrum are -5.43 and -3.17 eV, respectively. Optimized OSCs with a blend of SiF-BT:PC$_{71}$BM (3:6) exhibits a power conversion efficiency (PCE) of 0.53% with a short-circuit current density of -2.06 mA/cm^2, fill factor of 29.8%, and open-circuit voltage of 0.90 V.

Keywords: conjugated oligomer, silofluorene, benzothiadiazole, organic solar cell.

Introduction

Researches on organic solar cells have been increased due to their high promising low cost production and high performance that comes from organic semiconducting material. Organic semiconductors are promising materials to explore because of their potential applications in organic electronic devices, such as organic solar cells (OSCs), organic light-emitting diodes (OLEDs), and organic field-effect transistors (OFETs).[1] Among them, blending a semiconducting material

as the electron donor (D) and a soluble fullerene derivatives as the electron acceptor (A), bulk hetero-junctions (BHJs), present the efficient structure for OSCs because of broadened interfacial electron donor and electron acceptor contacting area in which D and A materials form interpenetrated networks.[2,3] Recently, conjugated oligomers based OSCs are continuously gaining attention as they offer several advantages and promising results for the OSCs. Compared with conjugated polymers, conjugated oligomers are highly pure, with well-defined structure and high degree of crystallinity,[4] which could improve fabrication reproducibility and prevent batch-to-batch variations.[5] Combining electron donor units with high HOMO/LUMO level and electron withdrawing units with low HOMO/
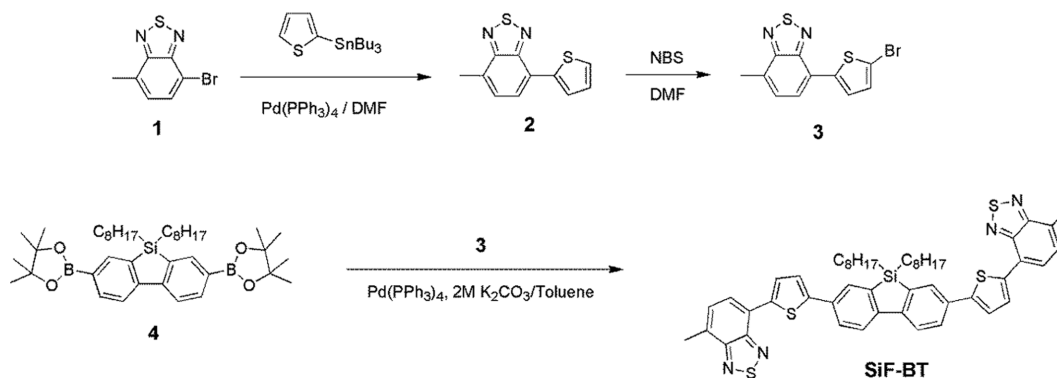
Scheme 1. Synthesis of SiF-BT and its chemical structure.

LUMO level is necessary to decrease the band gap.[6] Most of electron donor units are alkylated fused-ring derivatives[7,8] based on fluorene,[9-11] carbazole,[12-15] and thiophene.[16,17] Oligomers based on fluorene moiety have been studied in organic electronic devices due to their stable thermal and chemical stability,[18] high molar extinction coefficients and efficient light harvesting properties could be great potential to increase the power conversion efficiency (PCE).[19] Silofluorene (SiF) is gaining attention due to their unique electronic structure and has a low lying LUMO.[20] Another advantage is silicon atom can stabilize the HOMO levels compared to the carbon counterparts.[21] For the electron withdrawing moiety, 2,1,3-benzothiadiazole derivatives are commonly used as the A because coupling with D units especially in the BHJ solar cells exhibits the high PCE.[22] We synthesized an A-D-A type oligomer containing a central SiF unit as the electron D and 2,1,3-benzothiadiazole (BT) derivative as the electron A as their implementation as donor material in organic solar cells, which is 2,7-bis[5-(7-methyl-benzo[1,2,5] thiadiazol-4-yl)-thiophen-2-yl]-9-(9,9-dioctyl)-9H-silofluorene (SiF-BT) (Scheme 1). Here, we report the synthesis, characterization, optical properties, and photovoltaic properties of OSCs based on SiF-BT.

Experimental

Materials. PC$_{71}$BM (Cat No. nano-cPCBM-SF) was purchased from nano-C, Inc. 4-bromo-7-methyl-benzo[1,2,5]thiadiazole (1)[23] and 2,7-dibromo-9,9-dioctyl-9H-dibenzosilole (4)[24,25] were synthesized according to the literature procedures.

Synthesis of 4-methyl-7-thiophen-2-yl-benzo[1,2,5]thiadiazole (2). Synthesis of compound 2 was followed by the general procedure for the Stille coupling reaction. A mixture of compound 1 (4.582 g, 20.00 mmol), tributyl-thiophen-2-yl-stannane (8.956 g, 24.00 mmol) and 3.0 mol% of tetrakis (triphenylphosphine) palladium [Pd(PPh$_3$)$_4$] (0.693 g, 0.600 mmol) in N,N-dimethylformamide (DMF) was stirred for 24 h at 90 °C under N$_2$ atmosphere. A portion of 100 mL of water was added the mixture and allowed to cool to room temperature. The mixture was extracted with ethyl acetate (EA) and the extracted organic layer was dried over anhydrous MgSO$_4$. The organic solvent was removed by using a rotary evaporator. The crude product was purified by column chromatography on silica gel using ethyl acetate (EA)/n-hexane. The yield of dark yellow solid was 4.820 g (77.9%). MS: [M$^+$], m/z 255. MS: [M$^+$], m/z 255. ^{1}H NMR (400 MHz, CDCl$_3$, ppm): δ 8.05~8.04 (dd, J_1 = 3.2 Hz, J_2 = 2.1 Hz, 1H), 7.76~7.74 (d, J = 6.9 Hz, 1H), 7.42~7.36 (m, 1H), 7.20~7.16 (dd, J_1 = 5.1 Hz, J_2 = 3.6 Hz, 1H), 2.75 (s, 3H). ^{13}C NMR (100 MHz, CDCl$_3$, ppm): δ 156.75, 152.82, 139.59, 130.35, 128.31, 127.84, 126.93, 126.64, 125.86, 125.08, 17.92. Anal Calcd. For. C$_{11}$H$_8$N$_2$S$_2$: C, 56.87; H,3.47; N, 12.06; S 27.60. Found: C, 56.54; H, 3.34; N, 12.03; S, 27.43.

Synthesis of 4-(5-bromo-thiophen-2-yl)-7-methyl-benzo [1,2,5]thiadiazole (3). A mixture of compound (2) (4.660 g, 20.00 mmol) and N-bromosuccinimide (4.272 g, 24.00 mmol) in N,N-dimethylformamide (DMF) was stirred for 24 h at 90 °C under N$_2$ atmosphere. A portion of 100 mL of water was added the mixture and allowed to cool to room temperature. The mixture was extracted with methylene chloride (MC) and the extracted organic layer was dried over anhydrous MgSO$_4$. The organic solvent was removed by using a rotary evaporator. The crude product was purified by recrystallization using methanol. The yield of yellow powder was 4.759 g (85.1%). MS: [M$^+$], m/z 334. ^{1}H NMR (400 MHz, CDCl$_3$, ppm): δ 7.74~7.73 (d, J = 4.1, 1H), 7.69~7.67 (d, J = 7.3 Hz, 1H), 7.38~7.36 (dd, J_1 = 5.3 Hz, J_2 = 1.1 Hz, 1H), 7.13~7.12 (d, J = 4 Hz,

1H), 2.74 (s, 3H). ^{13}C NMR (100 MHz, CDCl$_3$, ppm): δ 156.25, 153.44, 140.06, 138.37, 130.50, 128.28, 127.94, 126.63, 126.04, 125.31, 17.96. Anal Calcd. For. C$_{11}$H$_7$BrN$_2$S$_2$: C, 42.45; H, 2.27; N, 9.00; S, 20.61. Found: C, 42.37; H, 2.20; N, 9.16; S, 20.28.

Synthesis of 2,7-bis[5-(7-methyl-benzo[1,2,5]thiadiazol-4-yl)-thiophen-2-yl]-9-(9,9-dioctyl)-9H-silofluorene (SiF-BT). A mixture of compound (3) (0.747 g, 2.40 mmol) (9-(9,9-dioctyl)-2,7-bis-(4,4,5,5-tetramethyl-[1,3]dioxolan-2-yl)-9H-silofluorene (0.658 g, 1.00 mmol), 5% mol of tetrakis(triphenyl-phospine) palladium [Pd(PPh$_3$)$_4$] (0.058 g, 0.050 mmol), and several drops of aliquat. 336 in 20 mL of degassed 1:1 (by volume) mixed solvent of toluene and 2 M K$_2$CO$_3$ aqueous was stirred for 12 h at 75 °C under the N$_2$. A portion of 100 mL of water was added the mixture and allowed to cool to room temperature. The mixture was extracted with EA and the extracted organic layer was dried over anhydrous MgSO$_4$. The organic solvent was removed by using a rotary evaporator. The crude product was purified by column chromatography on silica gel using EA/n-hexane. The yield of dark orange solid was 0.528 gr (60.9%). Mp: 137 °C. MS: [M$^+$], m/z 889. ^{1}H NMR (400 MHz, CDCl$_3$, ppm) : δ 8.08~8.07 (d, J = 3.7 Hz, 1H), 7.94~7.93 (d, J = 1.5 Hz, 1H), 7.87~7.85 (d, J = 3.5 Hz, 1H), 7.82~7.79 (m, 2H), 7.47~7.46 (d, J = 3.6 Hz, 1H), 7.45~7.40 (dd, J_1 =7.3 Hz, J_2=1.1 Hz, 1H), 2.78 (s, 1H), 1.44~1.39 (m, 2H), 1.30~1.21 (m, 13H), 1.07~0.96 (m, 2H), 0.84~0.81 (m, 3H). ^{13}C NMR (100 MHz, CDCl$_3$, ppm): δ 155.94, 152.10 147.43, 145.05 138.96, 132.93, 130.37, 130.26, 128.41, 128.14, 127.64, 125.38, 125.06, 123.79, 121.36, 33.40, 31.86, 29.24, 29.11, 23.95, 22.65, 17.97, 14.10, 12.31. Anal Calcd. For. C$_{50}$H$_{54}$N$_4$S$_4$Si : C, 69.24; H, 6.28; N, 6.46; S, 14.79. Found: C, 69.13; H, 6.17; N, 6.87; S, 14.88.

Measurements. UV-Visible spectra were recorded using UV-Vis spectrophotometer (JASCO V-530). Cyclic voltammetry (CV) was performed by a an Ivium B14406 with a three electrode cell in a solution of 0.10 M tetrabutylammonium hexafluorophosphate (Bu$_4$NPF$_6$) in freshly distilled methylene chloride at a scan rate of 100 mV/s. Pt coil and wire were used as the counter and working electrode, respectively. An Ag/Ag$^+$ electrode was used as the reference electrode. Prior to each measurement, the cell was deoxygenated with nitrogen. The thickness of films was measured by an Alpha-Step IQ surface profiler (KLA-Tencor Co.). The J–V measurements under the 1.0 sun (100 mW/cm^2) condition from a 150 W Xe lamp with AM 1.5 G filter were performed using a KEITHLEY Model 2400 source-measure u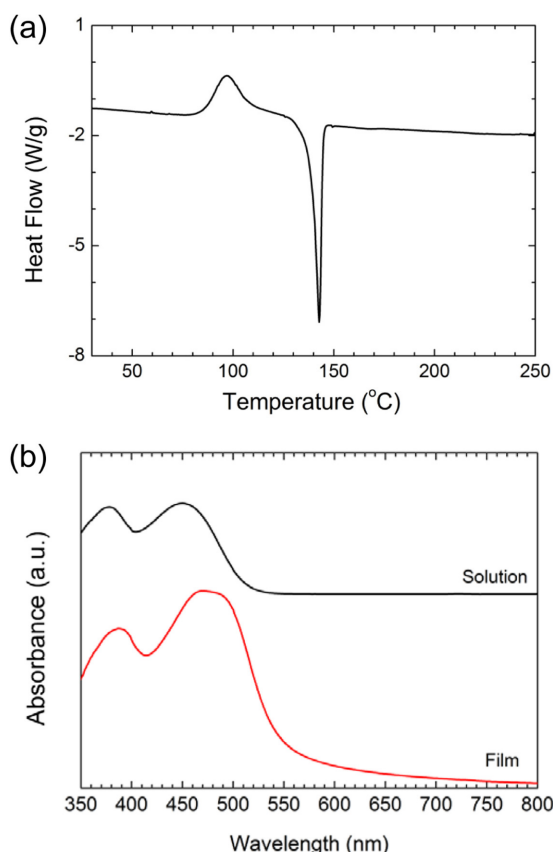nit. A calibrated Si reference cell with a KG5 filter certified by National Institute of Advanced Industrial Science and Technology was used to confirm the 1.0 sun condition. The atomic force microscopy (AFM) topography image was taken using a Bruker (NanoScope V) operated in the tapping mode.

Fabrication of PSCs. For fabrication of inverted type PSCs with a structure of ITO/ZnO/active layer (SiF-BT:PC$_{71}$BM)/MoO$_3$/Ag, a 25 nm-thick of ZnO film on ITO was deposited by using the sol-gel process. The sol-gel solution was prepared with 0.164 g of zinc acetate dihydrate and 0.05 mL of ethanolamine dissolved in 1 mL of methoxyethanol. The solution was stirred for 30 min at 60 °C prior to deposition. The thin film of ZnO precursor was cured at 200 °C for 10 min to partly crystallize the ZnO film. The active layer was spin-cast from the blend solution of donor and PC$_{71}$BM (donor and PC$_{71}$BM dissolve in 1 mL of chloroform at 600 rpm for 60 s). Prior to spin coating, the active solution was filtered through a 0.2 mm membrane filter. The typical thickness of an active layer was 80 nm. On the top of the active layer, a 20 nm-thick MoO$_3$ layer and 100 nm-thick Ag layer were thermally evaporated successively through a shadow mask with a device area of 0.13 cm^2 at 2×10^{-6} Torr.

Results and Discussion

Synthesis and Characterization of SiF-BT. As shown in Scheme 1, compound 2 was synthesized by the Stille coupling reaction between compound 1 and tributyl-thiophen-2-yl-stannane. SiF-BT was synthesized by the Suzuki coupling reaction between one equivalent of 2,7-dibromo-9,9-dioctyl-9H-dibenzosilole (4) and two equivalent of compound 3. Strong electron accepting and donating groups have been introduced to lower the band gap by the intramolecular charge transfer (ICT). The structures of all synthesized compounds were confirmed by ^{1}H NMR, ^{13}C NMR, elemental analysis (EA), and MASS. Thermal behavior was investigated by differential scanning calorimetry (DSC). Crystallization and melting process showed at 85 and 137 °C, respectively (Figure 1(a)). SiF-BT exhibits good solubility in chlorinated hydrocarbon solvents such as chloroform and chlorobenzene.
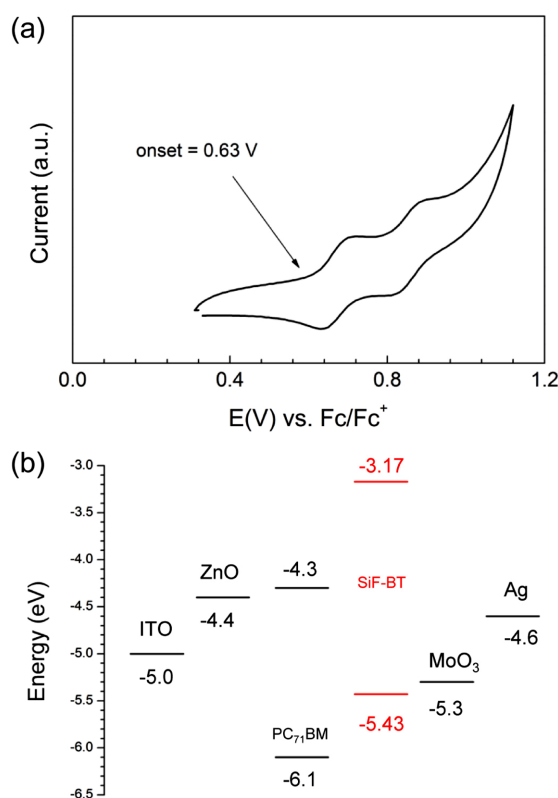
Figure 1(b) shows the UV-Visible spectra of SiF-BT in chloroform solution and in thin film. SiF-BT exhibit two broad absorption bands at a shorter wavelength region (shorter than 400 nm) and a longer wavelength region (410 ~ 600 nm). The former and latter correspond to π-π* transition and the typical intramolecular charge transfer (ICT), respectively.

(a)

(b)

Figure 1. (a) DSC thermogram; (b) UV-Visible spectrum of SiF-BT solution in chloroform and film.

(a)

(b)

Figure 2. (a) Cyclic voltammogram of SiBT-BT; (b) the energy level diagrams of the components in the device.

Table 1. Best Photovoltaic Parameters of OSCs. The Averages for the Photovoltaic Parameters of Each Device are Given in Parentheses
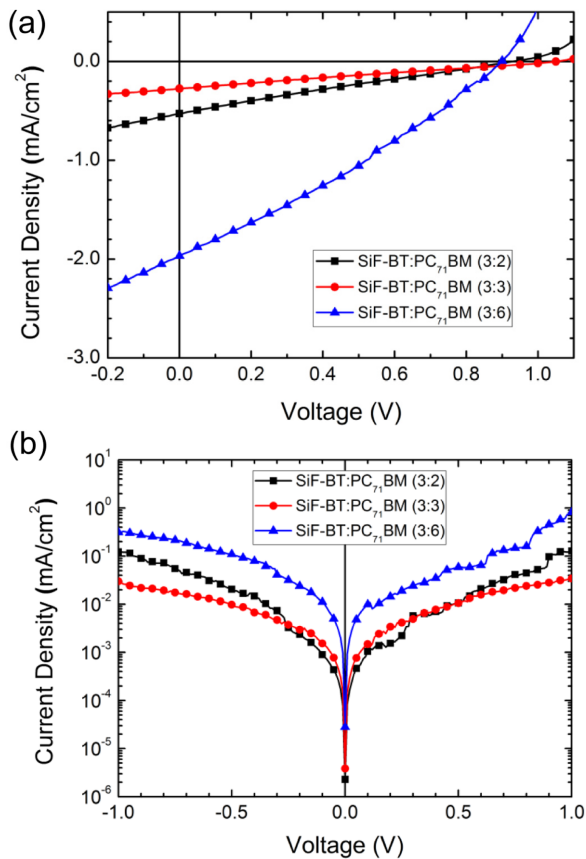
Blend ratio[a]	J_{sc} (mA/cm^2)	V_{oc} (V)	FF (%)	PCE (%)
3:3	0.31 (0.30)	0.97 (0.84)	22.1 (23.0)	0.07 (0.06)
3:6	1.30 (1.15)	0.91 (0.85)	31.0 (29.1)	0.37 (0.29)
3:9	1.13 (1.15)	0.85 (0.81)	31.9 (31.7)	0.31 (0.19)

[a]Mass ratio of donor to PC$_{61}$BM.

The absorption band of SiF-BT film at longer wavelength region are 20 nm red-shifted compared to that of solution, whereas the absorption maximum of film at shorter wavelength region film is almost identical to that of solution. A shoulder at 488 nm is appeared in the absorption spectrum of SiF-BT film, indicating the formation of the intermolecular aggregation, i. e. increase of molecular interaction in the solid state film. The molar extinction coefficients (ε) of SiF-BT is estimated to be 3.96×10^4 M^{-1} cm^{-1} in solution spectrum.

The HOMO energy level of SiF-BT was measured by cyclic voltammetry (CV). As shown in Figure 2(a), SiF-BT shows two reversible oxidation processes at 0.71 and 0.89 V *vs* ferrocene (Fc/Fc$^+$). From the oxidation onset potential, the HOMO level of SiF-BT is estimated to be -5.43 eV. The optical band gap energy was estimated from the absorption edge of SiF-BT film (548 nm), which corresponds to 2.26 eV. Even though two thiophene rings are introduced as the π-extender, SiF-BT exhibits a pretty wide band gap. This may due to weak ICT between SiF and BT. The LUMO energy level of SiF-BT was calculated using the HOMO energy level and the optical band gap

obtained from UV-visible absorption edge was -3.17 eV. The energy levels of SiF-BT, PC$_{71}$BM and other materials used in this research were illustrated in Figure 2(b). They can provide sufficient driving forces for the efficient operation of solar cells through the facile exciton dissociation as well as energetically favored charge transfer process.

Photovoltaic Properties. Performances of OSCs based on SiF-BT and PC$_{71}$BM (or PC$_{61}$BM) were measured in the inverted type OSCs with a structure of ITO/ZnO (25 nm)/

donor: $PC_{71}BM$ (or $PC_{61}BM$)/MoO_3 (20 nm)/Ag (100 nm). In order to optimize device test and fabrication conditions, the photovoltaic parameters (Table 1) were preliminary tested with different blend ratios of SiF-BT and $PC_{61}BM$ from 3:3 to 3:9 (w/w). On the basis of the testing results, we fabricated and

tested the devices with blend ratio of SiF-BT and $PC_{71}BM$ from 3:2 to 3:6 (w/w). The current density (J) – voltage (V) curves of the devices under AM 1.5 G simulated illumination are shown in Figure 3(a) and the photovoltaic parameters are summarized in Table 2.

The PCE of the devices were 0.12~0.53%, which depends on the blend ratio. In addition, the V_{oc}, J_{sc}, and FF of the devices were 0.90~1.01 V, 0.53~2.06 mA/cm^2, and 23.4~29.8%, respectively. The best blend ratio between SiF-BT and $PC_{71}BM$ having the best PCE appeared at 3:6. The series resistance (R_s)[26] was calculated from the inverse slope near the high current regime of the $J - V$ curves under dark condition and the results were listed in Table 2. The R_s data are good correlated with the PCE and the FF data of the devices.

To investigate charge transporting properties of the active layer through the space charge limited current (SCLC) methods, the hole- and electron-only devices with a structure of ITO/PEDOT:PSS (35 nm)/SiF-BT:$PC_{71}BM$ (3:6) (80~120 nm)/ Au (50 nm) and ITO/ZnO (25 nm)/SiF-BT:$PC_{71}BM$ (3:6) (70~ 100 nm)/Al (100 nm), respectively, were prepared. Above the built-in electric field (as shown in Figure 4), the current density

Figure 3. Current density-voltage curves of BHJ type OPVs based on SiF-BT and $PC_{71}BM$ at different weight ratio under (a) AM 1.5G simulated illumination with an intensity of 100 mW/cm^2; (b) the dark condition.

Table 2. Best Photovoltaic Parameters of OSCs. The Averages for the Photovoltaic Parameters of Each Device Are Given in Parentheses
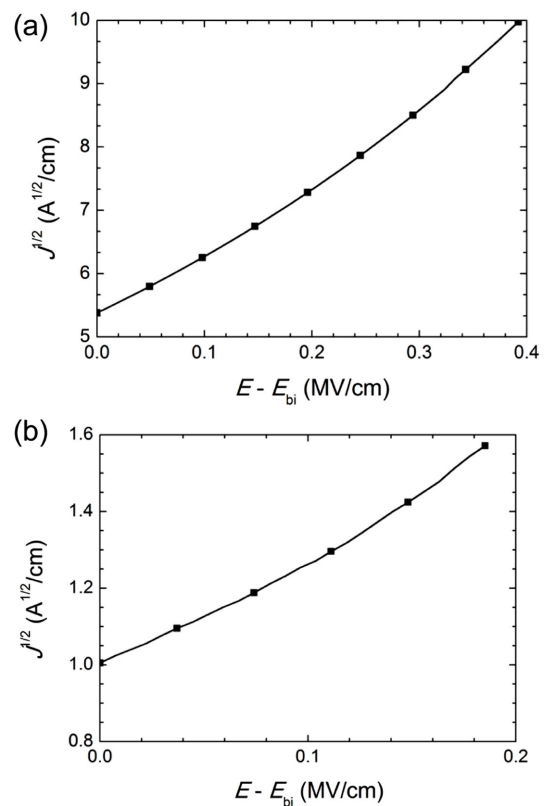
Blend ratio[a]	J_{sc} (mA/cm^2)	V_{oc} (V)	FF (%)	PCE (%)	R_s ($\Omega\ cm^2$)[b]
3:2	0.53 (0.50)	1.01 (0.97)	23.4 (23.3)	0.12 (0.11)	35.2
3:3	0.28 (0.27)	1.05 (1.04)	24.0 (24.2)	0.07 (0.07)	38.1
3:6	2.06 (1.99)	0.90 (0.84)	29.8 (30.9)	0.53 (0.51)	25.2

[a]Mass ratio of donor to $PC_{71}BM$. [b]Series resistance, respectively (estimated from the corresponding best device).

Figure 4. Current density–voltage curve of (a) hole-only device; (b) electron-only device based on SiF-BT:$PC_{71}BM$ (3:6).
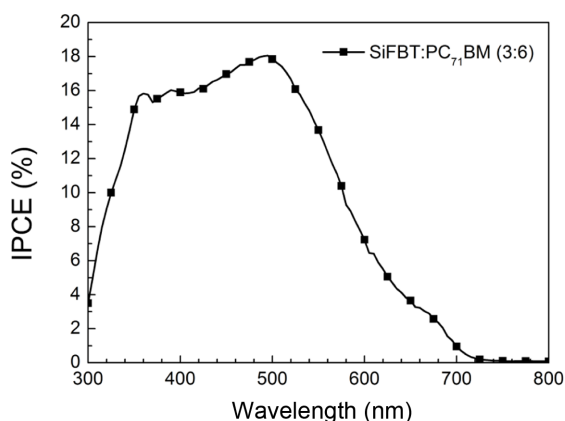
Figure 5. IPCE spectra of OSC based on SiF-BT:PC$_{71}$BM (3:6).

and electric field is characteristic of SCLC. This can be fitted by the Mott-Gurney law;[27]

$$J = \frac{9}{8}\varepsilon_0\varepsilon_r\mu\frac{E^2}{L}$$

where J is the current density, μ is the charge mobility, E is the electric field, $\varepsilon_0\varepsilon_r$ is the permittivity the active layer, L is the thickness of the active layer, respectively. Using ε_r=3.9,[27] the current density and electric field relationship of the device agree well with Mott-Gurney Law. The hole and electron mobility of the device are 2.02×10^{-4} and 1.58×10^{-5} cm^{2}V^{-1}s^{-1}, respectively.

Incident photon conversion efficiency (IPCE) was measured for the corresponding best device to verify the accuracy of the measurements. As shown in Figure 5, the devices show typical IPCE curves from 300 to 800 nm. The maximum IPCE of the device with SiF-BT:PC$_{71}$BM (3:6) shows at 490 nm. Estimated J_{sc} value from the IPCE spectra is 2.23 mA/cm^2, which is agree well with the J_{sc} value of under the 1.0 sun condition.

Conclusions

A new A-D-A type conjugated small molecule based on 2,1,3-benzothiadiazole and silofluorene (SiF-BT) has been synthesized successfully. According to the DSC thermogram, crystallization and melting process showed at 85 and 137 °C, respectively. Glass transition process did not appear up to 200 °C. All the compounds in this research were well characterized by NMR, MASS, and EA. Even though two thiophene rings are introduced as the π-extender, SiF-BT exhibits a wide band gap of 2.26 eV. The HOMO and LUMO energy levels of SiF-BT figured out from the CV and UV-Visible spectrum are -5.43 and -3.17 eV, respectively. Optimized OSCs with a blend of SiF-BT:PC$_{71}$BM (3:6) exhibit a power conversion efficiency (PCE) of 0.53% with a short-circuit current density of -2.06 mA/cm^2, fill factor of 29.8%, and open-circuit voltage of 0.90 V.

References

1. A. Mishra and P. Bäuerle, *Angew. Chem. Int.*, **51**, 2020 (2012).
2. C. D. Wessendorf, A. P. Rodriguez, J. Hanisch, A. P. Arndt, I. Ata, G. L. Schulz, A. Quintilla, P. Bäuerle, U. Lemmer, P. Wochner, E. Ahlswede, and E. Barrena, *J. Mater. Chem.*, **4**, 2571 (2016).
3. C. Zhou, Y. Liang, F. Liu, C. Sun, X. Huang, Z. Xie, F. Huang, J. Roncali, T. P. Russel, and Y. Cao, *Adv. Func. Mater.*, **24**, 7538 (2014).
4. L. Yuan, Y. Zhao, J. Zhang, Y. Zhang, L. Zhu, K. Lu, W. Yan, and Z. Wei, *Adv. Mater.*, **27**, 4229 (2015).
5. R. Fitzner, E. Mena-osteritz, A. Mishra, G. Schulz, E. Reinold, M. Weil, C. Korner, H. Ziehlke, C. Elschner, K. Leo, M. Riede, M. Pfeiffer, C. Uhrich, and P. Bäuerle, *J. Am. Chem. Soc.*, **134**, 11064 (2012).
6. J. Ku, Y. Lansac, and Y. H. Jang, *J. Phys. Chem. C*, **115**, 21508 (2011).
7. G. Park, I. Ryu, and S. Yim, *Bull. Korean Chem. Soc.*, **32**, 943 (2011).
8. G. Tregnago, T. T. Steckler, O. Fenwick, M. R. Andersson, and F. Cacialli, *J. Mater. Chem. C*, **3**, 2792 (2015).
9. G. Marzari, J. Durantini, D. Minudri, M. Gervaldo, L. Otero, F. Fungo, G. Pozzi, M. Cavazzini, S. Orlandi, and S. Quici, *J. Phys. Chem. C*, **116**, 21190 (2012).
10. P. C. Rodrigues, L. S. Berlim, D. Azevedo, N. C. Saavedra, P. N. Prasad, W. H. Schreiner, T. D. Z. Atvars, and L. Akcelrud, *J. Phys. Chem. A*, **116**, 3681 (2012).
11. D. Mori, H. Benten, H. Ohkita, S. Ito, and K. Miyake, *ACS Appl. Mater. Interfaces*, **4**, 3325 (2012).
12. A. Michaleviciute, M. Degbia, A. Tomkeviciene, and B. Schmaltz, *J. Power Sources*, **253**, 230 (2014).
13. J. Lu, P. F. Xia, P. K. Lo, Y. Tao, and M. S. Wong, *Chem. Mater.*, **18**, 6194 (2006).
14. N. Blouin, A. Michaud, D. Gendron, S. Wakim, M. Blair, R. Neagu-Plesu, M. Belletete, G. Durocher, Y. Tao, and M. Leclerc, *J. Am. Chem. Soc.*, **130**, 732 (2008).
15. T. Sudyoadsuk, S. Pansay, S. Morada, R. Rattanawan, S. Namuangruk, T. Kaewin, S. Jungsuttiwong, and V. Promarak, *Eur. J. Org. Chem.*, 5051 (2013).

16. J. B. Kim, K. Allen, S. J. Oh, S. Lee, M. F. Toney, Y. S. Kim, C. R. Kagan, C. Nuckolls, and Y. L. Loo, *Chem. Mater.*, **22**, 5762 (2010).

17. S. Haid, A. Mishra, C. Uhrich, M. Pfei, and P. Bäuerle, *Chem. Mater.*, **23**, 4435 (2011).

18. N. A. D. Yamamoto, L. L. Lavery, B. F. Nowacki, I. R. Grova, G. L. Whiting, B. Krusor, E. R. Azevedo, L. Akcelrud, A. C. Arias, and L. S. Roman, *J. Phys. Chem. C*, **116**, 18641 (2012).

19. D. Kumar, K. R. J. Thomas, C. Lee, and K. Ho, *J. Org. Chem.*, **79**, 3159 (2014).

20. H. Huang, J. Youn, R. P. Ortiz, Y. Zheng, A. Facchetti, and T. Marks, *Chem. Mater.*, **23**, 2185 (2011).

21. S. Yamaguchi and K. Tamao, *Bull. Chem. Soc. Jpn.*, **69**, 2327 (1996).

22. S. Song, H. I. Choi, I. S. Shin, M. H. Hyun, H. Suh, S. S. Park, S. H. Park, and Y. Jin, *Bull. Korean Chem. Soc.*, **35**, 2963 (2014).

23. M. Jorgensen and F. C. Krebs, *J. Org. Chem.*, **70**, 6004 (2005).

24. K. L. Chan, M. J. McKiernan, C. R. Towns, and A. B. Holmes, *J. Am. Chem. Soc.*, **127**, 7662 (2005).

25. W. Shin, J. H. Park, G. E. Lim, N. Sylvianti, B. H. Ahn, and J. H. Kim, *Synth. Met.*, **210**, 201 (2015).

26. J. Xue, S. Uchida, B. P. Rand, and S. R. Forrest, *Appl. Phys. Lett.*, **84**, 3013 (2004).

27. V. D. Mihailetchi, J. K. Van Duren, P. W. Blom, J. C. Hummelen, R. A. Janssen, J. M. Kroon, M. T. Rispens, W. J. H. Verhees, and M. M. Wienk, *Adv. Funct. Mater.*, **13**, 43 (2003).